Radiol med (2016) 121:769–779
DOI 10.1007/s11547-016-0660-3

CHEST RADIOLOGY

Flat detector cone-beam CT-guided percutaneous needle biopsy of mediastinal lesions: preliminary experience

Dechao Jiao[1] · Kai Huang[2] · Gang Wu[1] · Yanli Wang[1] · Xinwei Han[1]

Received: 7 March 2016 / Accepted: 30 May 2016 / Published online: 22 June 2016

Abstract
Purpose The purpose of this study was to evaluate the usefulness of flat detector cone-beam CT-guided CBCT percutaneous needle biopsy (PNB) of mediastinal lesions.
Methods A total of 100 patients with 100 solid mediastinal lesions were retrospectively enrolled to undergo percutaneous needle biopsy (PNB) procedures. The mean diameter of lesions was 4.4 ± 1.8 cm (range 1.8–9.0 cm). The needle path was carefully planned and calculated on the CBCT virtual navigation guidance system, which acquired 3D CT-like cross-sectional images. Diagnostic performance, procedure details, complication rate, and patient radiation exposure were investigated.
Results The technical success rate of PNB under CBCT virtual navigation system was 100 % (100/100). The sensitivity, specificity, and accuracy of PNB of small nodules under iGuide CBCT virtual navigation guidance were 95.1 % (79/83), 100 % (12/12), and 95.7 % (91/95), respectively. The number of biopsies and CBCT acquisitions were 2.6 ± 1.2 (range 1–6) and 3.0 ± 1.1 (range 2–8), respectively. Complications occurred in five (5.0 %) cases. The mean total procedure time was 11.70 ± 3.44 min (range 6–27 min), resulting in a mean exposure dose of 9.7 ± 4.3 mSv.
Conclusion Flat detector cone-beam CT-guided PNB is an accurate and safe diagnostic method for mediastinal lesions.

Keywords Interventional · Biopsy · Computer application-3D · Mediastinal lesion

✉ Xinwei Han
13592583911@163.com

Dechao Jiao
jiaodechao007@126.com

Kai Huang
7788675@qq.com

Gang Wu
wuganghenan2004@163.com

Yanli Wang
zzuwyl@sina.com

[1] Department of Interventional Radiology, The First Affiliated Hospital of Zhengzhou University, Zhengzhou 450052, Henan, People's Republic of China

[2] Department of Oncology, The First Affiliated Hospital of Zhengzhou University, Zhengzhou 450052, Henan, People's Republic of China

Introduction

Diagnostic discrimination of mediastinal tumors is crucial for planning appropriate treatment [1, 2]. Different pathological results lead to different treatments. For example, tumors, such as thymoma, are often treated with surgery, whereas lymphoma or metastatic lesions would be treated with chemotherapy or radiotherapy [3]. CT-guided percutaneous needle biopsy (PNB) has been widely performed in the diagnosis of mediastinal nodules [4, 5]. However, the conventional CT guidance has limitations in the lack of real-time monitoring and gantry tilting for a more accessible needle pathway to the target lesion [6, 7]. Along with the development of flat detector cone-beam CT (CBCT), a novel technique for TNB guidance recently emerged. It combines advanced needle path planning with 3D CBCT images. The CBCT systems offer the real-time visualization of TNB procedures and more flexibility in the orientation of the detector system around the patient compared with the traditional CT systems [8, 9]. Therefore, the PNB

procedures assisted by advanced 3D needle guidance systems can be performed in a sterile workspace with flexible system angulation capability as well as instantaneous fluoroscopic feedbacks [10]. Indeed, owing to this system's ability to facilitate more accurate and safer needle placement, it has already been shown to provide excellent diagnostic accuracy for biopsy of the lung lesions [2, 8, 9, 11–19] (Table 1). However, there are few literatures about CBCT-guided percutaneous needle biopsy of mediastinal lesions [20]. This paper describes our preliminary experience with PNB for mediastinal lesions biopsy under the CBCT guidance system.

Methods and materials

Patients

This retrospective study was approved by the institutional review board of The First affiliated Hospital of Zhengzhou University with waiver of patient informed consent. From January 2010 to January 2015, a total of 100 patients with 100 solid mediastinal lesions were retrospectively enrolled to undergo PNB procedures. 100 consecutive patients (65 males and 35 females, mean age 52.00 ± 11.87 years; age range, 24–80 years) with enhanced CT or PET-CT confirmed solid mediastinal lesions were retrospectively enrolled in this study. The lesion size was recorded as the maximum diameter in the image data by one chest radiologist (Han XW, 20 years of experience in image-guided PNB).

Image acquisition

3D CBCT images of the patients were acquired with a rotational angiographic system (Artis Zeego, 30 × 40 cm FD detector, Siemens Healthcare, Forchheim Germany). The resulting raw projection images were then automatically transferred to a workstation (Syngo X Workplace, Siemens Healthcare) for 3D volume reconstruction. As a result, the CBCT images were reconstructed with 1 mm thickness and presented in axial, sagittal, and coronal orientations. The time from the end of the data acquisition to the presentation of multiplanar images on the workstation ranged between 43 and 45 s.

Needle path planning and guidance procedure

As the second step, the needle path was planned on the same workstation using the commercially available software (Syngo iGuide, Siemens Healthcare). Figures 1, 2 and 3 demonstrated this procedure for a 2.50 cm lesion in middle mediastinum. Figure 4 demonstrated this procedure for a 3.50 cm lesion in posterior mediastinum. Figure 5 demonstrated this procedure for a 1.80 cm lesion in middle mediastinum. The reconstructed 3D volume was first loaded. In the orthogonal multiplanar images, the skin entry point and target lesion positions were manually selected and marked by a cross and a circle, respectively. A virtual path was then generated with its angulations and length calculated and displayed. All three multiplanar images were automatically aligned to the defined path to provide in-plane views (Fig. 1b–d). Then, the virtual path was then projected and superimposed onto the live fluoroscopic images and displayed on a dedicated live monitor (Fig. 2). First, the C-arm rotated to the Bull's Eye View, where the C-arm was angulated in the way that the cross and the circle displayed on the live monitor completely matched and the central X-ray beam was aligned with the planned path (Fig. 2a). Thus, the skin entry point could be determined (Fig. 2a). The needle orientation was adjusted until both the tip and hub of the needle in the fluoroscopic image were superimposed and located at the center of the circle and the cross. Second, after the skin entry point and needle orientation were determined, the needle was advanced under fluoroscopy until the planned target lesion position was reached. The C-arm was rotated back and forth to two different angles subsequently to monitor the needle progression. These two angles provided lateral views (Progression View) of the planned needle path and helped to ensure that the needle was advanced along it (Figs. 2b, 5d). Third, a 3D scan was acquired to confirm the final position of the needle (Fig. 3).

PNB technique

PNBs were performed by or under the supervision of one chest radiologist (Han XW, 20 years of experience in image-guided PNB). Prior to the procedure, previously acquired diagnostic contrast-enhanced chest CT or PET-CT was carefully reviewed to determine the most appropriate needle route (Figs. 1a, 4a, 5a). The mean length of time from acquisition of the diagnostic CT image or PET-CT to the biopsy procedure was 7.6 ± 5.3 days (range 1–30 days). The patient was placed in either supine or prone position according to location of the lesion, and local anesthesia was given (1 % lidocaine, ≤10 ml). A 16-gauge needle (Quick-Core, Cook Medical Inc., Bloomington, IN, USA) was advanced along the planed path under real-time fluoroscopy. For sampling, the stylet was removed from the guiding needle and replaced by a biopsy needle, and then approximately 1.0–2.0 cm sample tissue was taken. A pathologist was not present, and our criteria were that the total samples length was more than 1.0 cm to meet the needs of the pathological sections. After sufficient tissue samples were obtained, the coaxial introducer was removed. Thereafter, post-procedure CT images were

Table 1 Recent studies on C-am cone-beam CT-guided biopsy procedures in the field of chest intervention

References	Year published	Biopsy target	Number of patients	Lesion size (cm)	Needle size (G)	Technical success rate (%)	Sensitivity (%)	Specificity (%)	Accuracy (%)	Complication rate (%)
Jin et al. [8]	2010	Lung nodule	71	≤3.0	18	100 (71/71)	97 (35/36)	100 (25/25)	98.4 (60/61)	Pneumothorax: 25.4 (18/71) Hemoptysis: 14.1 (10/71)
Hwang et al. [11]	2010	Lung nodule	27	≤2.0	20	100 (27/27)	94.1 (16/17)	88.9 (8/9)	92.3 (24/26)	Pneumothorax: 14.8 (4/27) Hemoptysis: 3 (1/27)
Cheung et al. [12]	2011	Lung nodule	74	≤3.0	20	100 (74/74)	90.6 (48/53)	100 (21/21)	93.2 (69/74)	Pneumothorax: 25.7 (19/74)
Choi et al. [13]	2012	Lung nodule	99	3.0 ± 1.6 (range 0.8–8.6)	18	100 (99/99)	95.8 (69/72)	100 (27/27)	97.0 (96/99)	Pneumothorax: 16.2 (16/99) Hemoptysis: 2 (2/99)
Lee et al. [14]	2012	Lung nodule	94	3.7 ± 2.3 (range 8–12)	20	100 (94/94)	93.1 (54/58)	100 (36/36)	95.7 (90/94)	Pneumothorax: 25.5 (24/94)
Choi et al. [15]	2012	Lung nodule	173	≤2.0	18	100 (173/173)	96.8 (91/94)	100 (69/69)	98.2 (160/163)	Pneumothorax: 31.8 (55/173) Hemoptysis: 14.5 (25/173)
Braak et al. [16]	2012	Lung nodule	84	3.25 (range 0.3–9.3)	18	100 (84/84)	90.0 (63/70)	100 (14/14)	91.7 (77/84)	Pneumothorax: 20.2 (17/84) Hemoptysis: 1.2 (1/84)
Choo et al. [17]	2013	Lung nodule	107	≤1.0	17	100 (107/107)	96.7 (58/60)	100 (38/38)	98.0 (96/98)	Pneumothorax: 6.5 (7/107) Hemoptysis: 5.6 (6/107)
Lee et al. [9]	2014	Lung nodule	1153	2.7 ± 1.7 (range 0.5–13.0)	20	99.6 (1148/1153)	95.7 (733/766)	100 (323/323)	97.0 (1056/1089)	Pneumothorax: 17.0 (196/1153) Hemoptysis: 6.9 (80/1153)
Floridi et al. [18]	2014	Lung nodule	100	5.19 (range 0.7–14)	20	95 (95/100)	91.2	100	92.5	Pneumothorax:21 % (20/95)
Rotolo et al. [19]	2015	Lung nodule	113	≤3.0	20	91.8 (113/123)	87	100	89	Pneumothorax: 29.3 (36/123) Hemoptysis: 27.9 (27/123)
Jiao et al. [2]	2015	Lung nodule	100	≤2.0	18	99 (99/100)	98.7	90.5	97	Pneumothorax: 10.1 (10/99) Hemoptysis:12.1 (12/99)

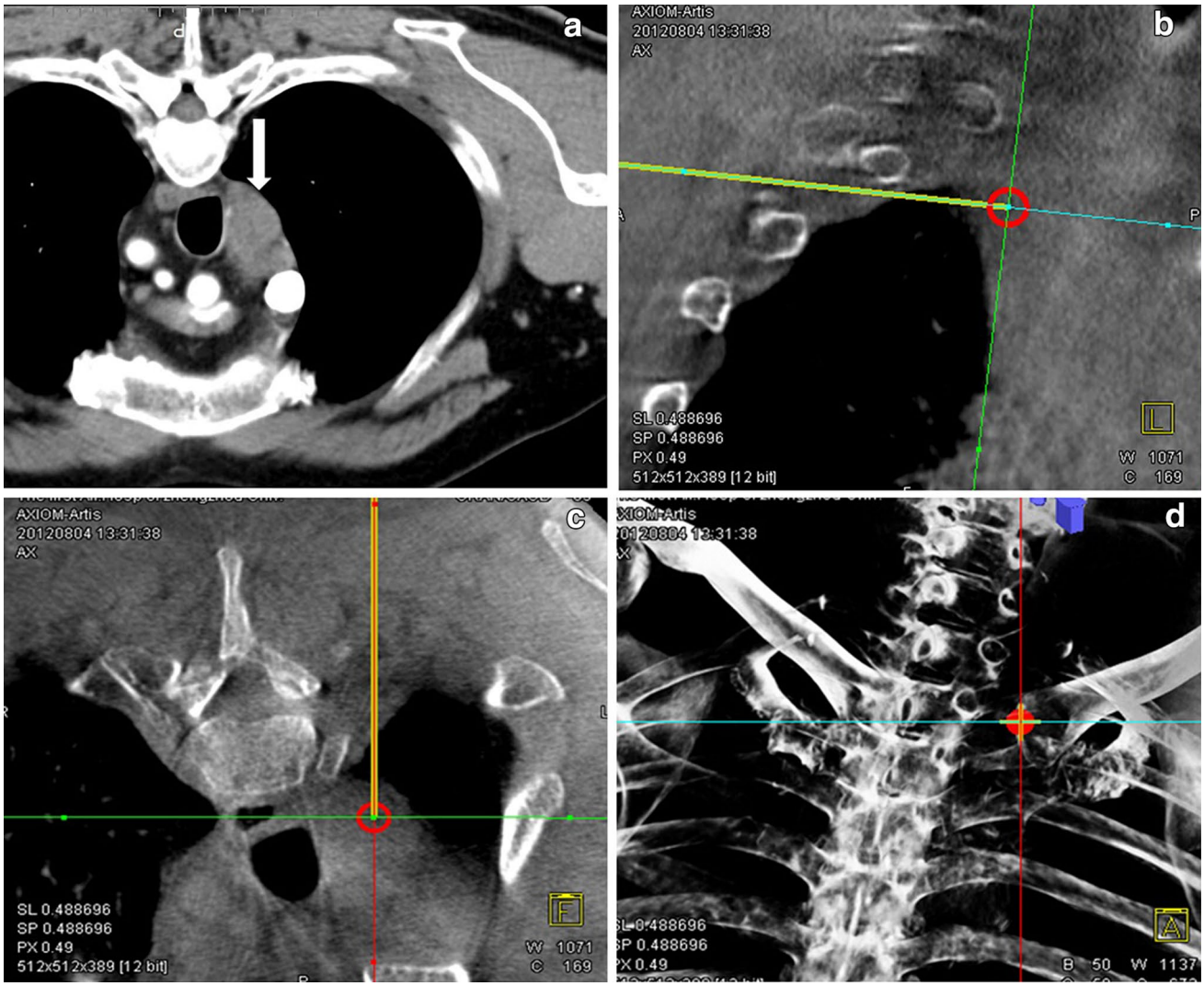

Fig. 1 55-year-old patient, preoperative CT showed a 2.50 cm middle mediastinal lesion (*white arrow*) (**a**). CBCT orthogonal multiplanar images with graphics showing planned needle path (*yellow line*) into target lesion (*red circle*) (**b**, **c**). The *cross* indicated the skin entry site, and the *circle* indicated the target lesion site. The needle position relative to the anatomical structures was displayed in 3D using the volume-rendering technique (**d**)

acquired to identify procedure-related complications. The patients remained in the hospital for 24 h for observation after the procedure.

Lesion characteristics and procedural records

Operators documented lesion characteristics as well as the procedural records in our database. We recorded the lesion size, location in the mediastinum, and lesion feature (solid, cystic, or mixed solid and cystic). We recorded several factors during TNB; the patients' positions during PNB, skin-to-target distance, the number of biopsies, the number of CT acquisitions, needle approach, total procedure time (defined as the duration from local anesthesia injection to the end of post-procedure CBCT). Technical success was defined as appropriate location of the coaxial needle within target nodules on CBCT images and adequate tissue sampling on visual inspection. We recorded the total coaxial introducer indwelling time and effective radiation exposure dose during the entire procedure (fluoroscopy dose and CBCT dose).

Pathological results, diagnostic accuracy

The pathological reports of biopsy specimens, surgical specimens, or follow-up images were reviewed to evaluate the final diagnosis of target nodules. Final diagnosis was confirmed in four ways. (1) If the patient underwent surgical resection, the pathological report decided the final diagnosis. (2) If the pathological result of biopsy demonstrated

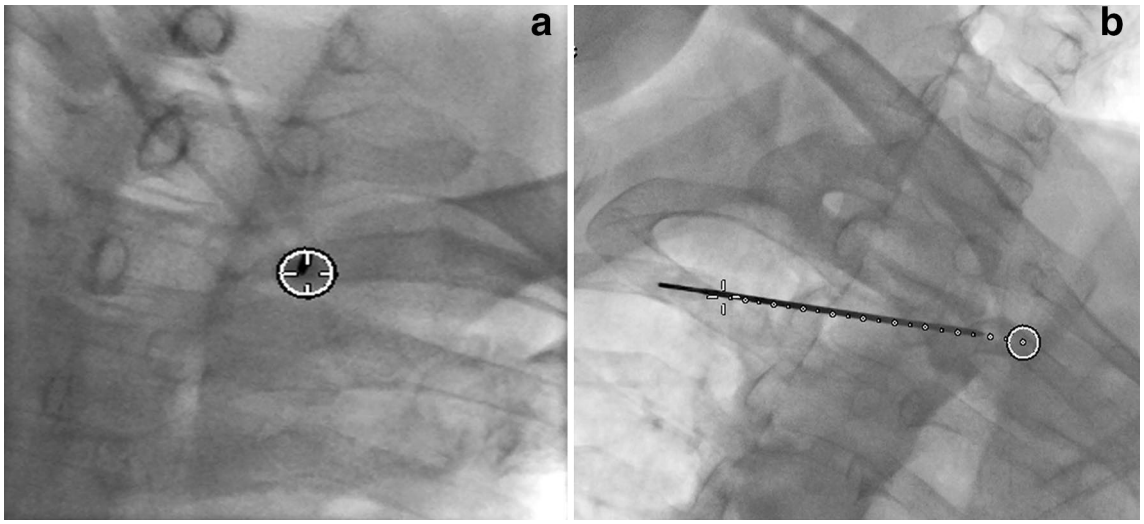

Fig. 2 Real-time fluoroscopic images in Bull's eye view (**a**) and progression views (**b**). The needle was advanced along the planned needle path (*dotted line*) from skin entry site (*white cross*) to target lesion site (*white circle*)

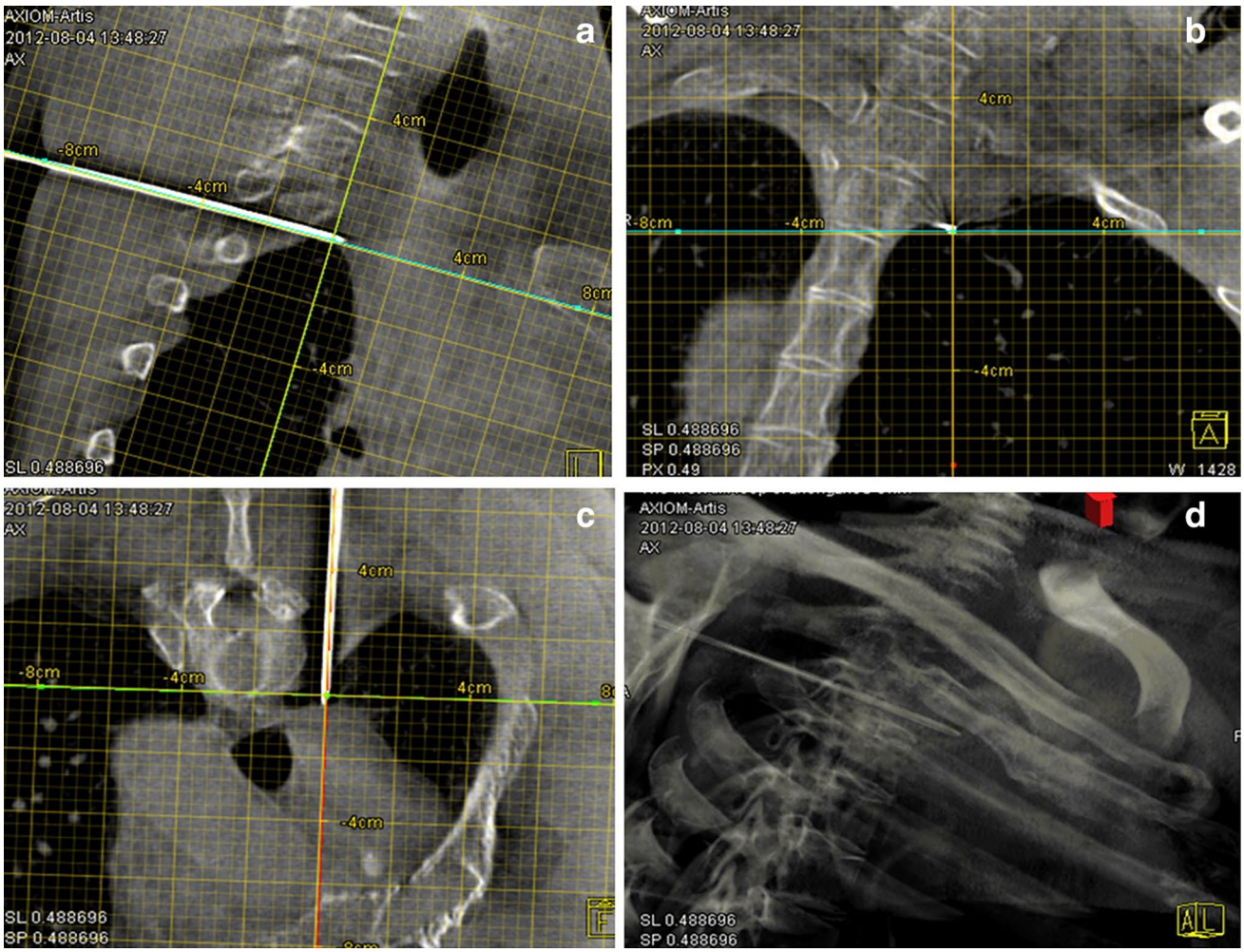

Fig. 3 CBCT scan confirmed the needle position in multiplanar (**a**–**c**) and volume-rendering (**d**) images

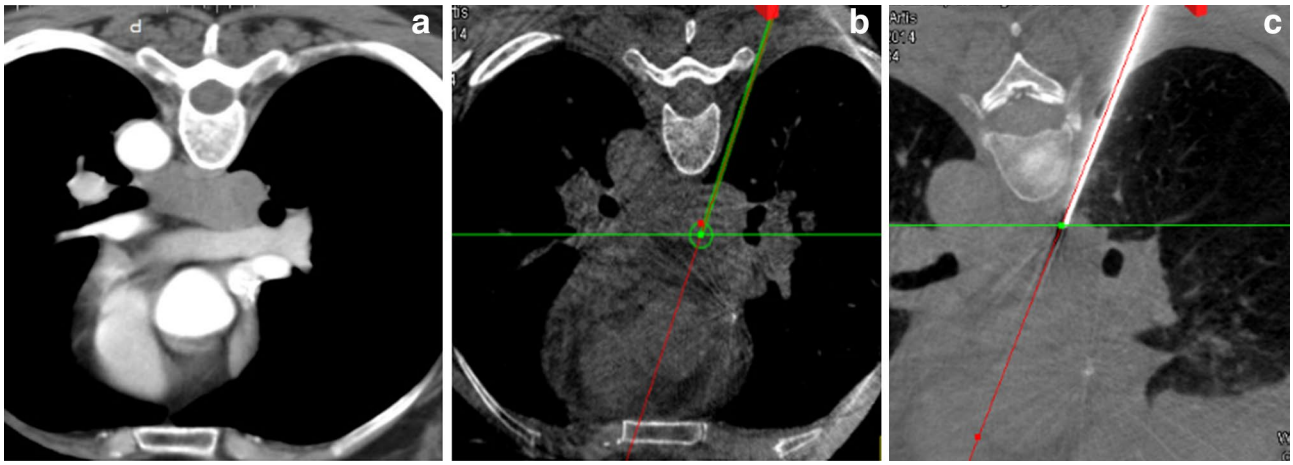

Fig. 4 58-year-old patient, preoperative CT showed a 3.5 cm lesion in posterior mediastinum (**a**). CBCT images with graphics showing planned needle path (*green line*) into target lesion (*green circle*) (**b**). CBCT scan confirmed the needle position (**c**)

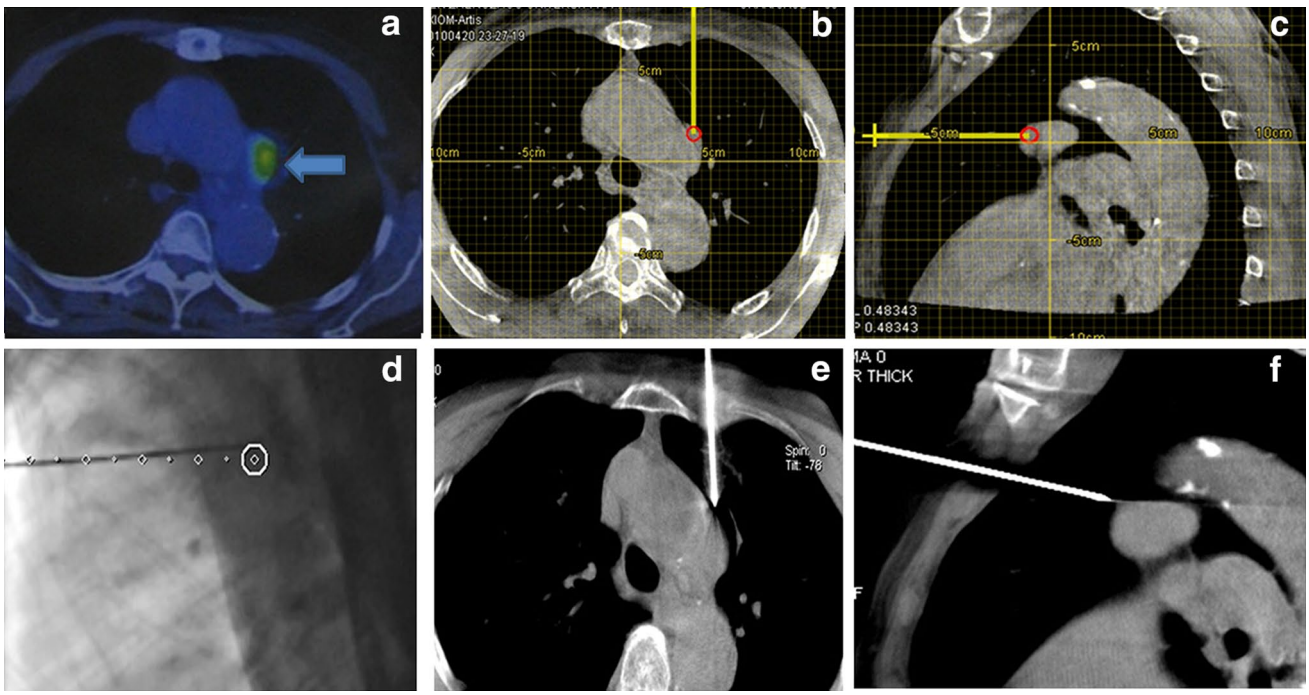

Fig. 5 80-year-old patient, preoperative PET-CT showed a 1.8 cm lesion in middle mediastinum (**a**). CBCT orthogonal multiplanar images with graphics showing planned needle path (*yellow line*) into target lesion (*red circle*) (**b**, **c**). Real-time fluoroscopic images in progression views, the needle was advanced along the planned needle path (*dotted line*) (**d**). CBCT scan confirmed the needle position (**e**, **f**)

a malignant or a specific benign pathology, such as thymoma or sarcoidosis, it was accepted as the final diagnosis. (3) In the cases of non-specific benign pathology (negative for malignancy, chronic inflammation, etc.), follow-up CT helped to decide whether the lesion would be truly or falsely benign, or indeterminate. If the lesion decreased 20 % or more in diameter, we considered the final diagnosis as benign. (4) If a nodule of non-specific benign pathology did not show a sufficient interval decrease in size nor had follow-up images, its final diagnosis was defined as indeterminate. Interminate lesions were not included in the calculation of diagnostic accuracy. Any PNB-related complication, such as pneumothorax or haemoptysis, was also recorded. Pneumothorax was evaluated with post-procedural CBCT and follow-up chest radiographs during the hospitalization.

All data analyses were performed using the Excel 2010 (Microsoft, Redmond, WA) and SPSS software (version

Table 2 Lesion characteristics and procedure records of flat detector cone-beam CT-guided percutaneous needle biopsy of mediastinal lesions

Data collection	Value
Total no. of patient	100
Lesion diameter (cm)	4.41 ± 1.75
Location of the lesion	
Anterior mediastinum	76
Middle mediastinum	12
Posterior mediastinum	12
Lesion feature	
Solid	81
Cystic	2
Mixed	17
Patient position	
Supine	85
Prone	15
Approach technique	
Patasternal	78
Transpulmonary	10
Paravertebral	12
Number of biopsies	2.59 ± 1.17
Number of CBCT acquisition	2.95 ± 1.11
Procedure time (min)	11.70 ± 3.44
Needle dwelling time (min)	8.20 ± 3.40
Effective dose (mSv)	9.7 ± 4.3

13.0; SPSS, Chicago). Numeric data are reported as the mean ± standard deviation.

Results

Nodule characteristics, procedural records, and radiation doses

A detailed description of the lesion characteristics and procedure records is summarized in Table 2. The mean size of nodules was 4.4 ± 1.8 cm, ranging from 1.8 cm to 9.0 cm. Among the 100 nodules, 81 lesions were solid, 2 lesions were cystic, and 17 showed mixed solid and cystic features. 76 lesions were located in the anterior mediastinum, 12 lesions in the middle mediastinum, and 12 in the posterior mediastinum. The patients underwent TNB in the supine position in 85 cases and in the prone position in 15 cases. The number of biopsies and CBCT acquisitions were 2.6 ± 1.2 (range 1–6) and 3.0 ± 1.1 (range 2–8), respectively. The mean total procedure time was 11.7 ± 3.4 min (range 6–27 min). With regard to the mediastinal needle approach used, the parasternal approach was used for 78 lesions, the paravertebral approach for 12 lesions, and transpulmonary approach for 10 lesions. The technical success rate of TNB under iGuide CBCT virtual navigation system was 100.0 % (100/100). The total coaxial introducer

Table 3 Pathologic outcomes of the patients who underwent PNB procedure with Siemens CBCT needle guidance system

The technical success rate (%)	100				
Sensitivity (%)	95.2				
Specificity (%)	100				
Accuracy (%)	95.7				
Pneumothorax rate (%)	3				
Subcutaneous hematoma	1				
Hemoptysis rate (%)	1				
Malignant	83	Benign	12	Indeterminate lesions	5
Thymoma	22 (26.5)	Chronic granulomatous	3 (25.0)	No enough evidence	2
Non-hodgkin's lymphoma	17 (20.5)	Fibroma	3 (25.0)	Lost to follow-up	3
Thymic carcinoma	11 (13.3)	Mature teratoma	2 (16.8)		
Metastases	10 (12.1)	Sarcoidosis	1 (8.3)		
Hodgkin's disease	7 (8.4)	Schwannoma	1 (8.3)		
Thyroid carcinoma	5 (6.0)	Inflammation with necrosis	1 (8.3)		
Malignant mesenchymal tumor	4 (4.8)	Tuberculosis	1 (8.3)		
Squamous cell carcinoma	3 (3.6)				
Fibrosarcoma	2 (2.4)				
Liposarcoma	2 (2.4)				

dwelling time in our study was 8.2 ± 3.4 min. The overall procedural time ranged from 6 to 27 min, and the mean total procedure time was 11.7 ± 3.4 min, resulting in a mean effective exposure dose of 9.7 ± 4.3 mSv.

Pathological results, diagnostic accuracy, and complications

Detailed pathological results are listed in Table 3. Among the 100 nodules, 83 nodules were malignant, 12 benign, and 5 indeterminate lesions. The final diagnosis of malignancy was made on the basis of surgical pathology ($n = 44$), including the conventional open surgery ($n = 24$) and endoscopic surgery ($n = 20$), and specific malignant biopsy results ($n = 39$). The 83 malignant lesions consisted of thymoma ($n = 22$), non-Hodgkin's lymphoma (NHL) ($n = 17$), thymic carcinoma ($n = 11$), metastases ($n = 10$), Hodgkin's disease (HD) ($n = 7$), thyroid carcinoma ($n = 5$), malignant mesenchymal tumor ($n = 4$), squamous cell carcinoma ($n = 3$), fibrosarcoma ($n = 2$), and liposarcoma ($n = 2$). The final diagnosis of benign lesions was made on the basis of surgical pathology ($n = 4$), including the conventional open surgery ($n = 2$) and endoscopic surgery ($n = 3$), and specific malignant biopsy results ($n = 7$). The 21 malignant lesions consisted of chronic granulomatous ($n = 3$), fibroma ($n = 3$), mature teratoma ($n = 1$), sarcoidosis ($n = 1$), Schwannoma ($n = 1$), inflammation with necrosis ($n = 1$), and tuberculosis ($n = 1$). One patients' initial biopsy result was fibrous connective tissue; the nodule was enlarged more than 20 % in size on follow-up chest CT after 2 months. TNB procedures were performed again, and the patient was confirmed with fibrosarcoma. The other three patients (one with HD and two with NHL) had completed the entire treatments, and tumor volumes were reduced more than 80 % compared with pretreatment. However, there were still persistence of soft tissue. Residual mediastinal tissue pathology results were coexists with fibrotic and/or necrotic tissue or thymic hyperplasia. Among them, two patients received the conventional open surgery and were confirmed with residual tumors. Another patent with NHL with high suspicion of tumor residue, TNB procedures were performed again, and the patient was confirmed with the residual tumor of NHL. Finally, the sensitivity, specificity, and accuracy of TNB of mediastinal lesions under the Siemens CBCT virtual navigation guidance were 95.1 % (79/83), 100 % (12/12), and 95.7 % (91/95), respectively.

Complications occurred in 5 of 100 procedures (5.0 %), all of which were pneumothorax ($n = 3$), subcutaneous hematoma ($n = 1$), and hemoptysis ($n = 1$). However, pneumothorax volume in every patient was below 5 %, and no specific treatment was given, as the patients were asymptomatic and clinically stable. Post-operative hemoptysis occurred in one patient, but the symptom was self-limiting and disappeared within 1 day. An old patient with giant mediastinal lesion (size 8.3 cm) and upper vena cava compression syndrome occurred subcutaneous hemorrhage after procedure. Puncture point was oppressed for 20 min, and bleeding was stopped.

Discussion

Imaging-guided PNB is regarded as an adequate technique for characterizing mediastinal lesions to be used before invasive surgical diagnostic procedures (mediastinoscopy, thoracoscopy, anterior mediastinotomy, and exploratory thoracotomy) [21]. CT-guided mediastinal lesion biopsy is well described in the literature with technical success ranging from 77 to 96.4 % [22–24]. The technical success rate of mediastinal lesion biopsy under CBCT virtual navigation was 100 % with accuracy rate 95.7 %, which falls within the aforementioned range. The favorable outcome achieved in our preliminary study suggested that the CBCT-guided biopsies can be as safe and accurate as CT-guided procedures. This finding is not surprising, because CBCT imaging guidance primarily affects the needle pass, but tissue sampling itself is essentially comparable to CT-guided procedures. Moreover, The CBCT systems offer real-time visualization on TNB procedures and more flexibility in the orientation of the detector system around the patient compared with the traditional CT systems [25]. Busser et al. [26] demonstrated that the CBCT was the preferred modality over CT, irrespective of the level of operator experience, in terms of accurate needle placement in difficult guidance procedures requiring double-angulated needle paths. As the mediastinum is a complex body part comprising the heart, trachea, esophageal, and multiple vascular structures, elaborate needle placement is essential. The study suggested that the CBCT virtual navigation-guided biopsy may be an exceptionally well-suited procedure for lesions in the mediastinum.

Several sampling methods are available. The simplest is fine-needle-aspiration cytology, which uses 20- to 25-gauge needles and provides a cytological sample consisting of exfoliated cells. Another sampling system is core biopsy, which relies on the use of special semiautomatic or automatic cutting needles with a quick-release mechanism and a 14- to 18-gauge caliber. This system provides microhistological samples (frustules). The larger amount of tissue harvested allows sophisticated laboratory investigations, such as electronic microscopy, immunohistochemistry, and tumor-marker analysis, and all factors improve diagnostic specificity [27]. Considering the diversity of the mediastinum tumors and classification necessity of lymphomas, we used 16-gauge biopsy needle advancing along the planed

path under real-time fluoroscopy to get enough sample, even if the lesion closed to blood vessels (Fig. 5). The real-time imaging CBCT guidance can make the biopsy procedures faster, and the total coaxial introducer dwelling time in our study was only 11.7 ± 3.4 min, which was shorter than that under the conventional CT guidance (mean 14.4–23.8 min) [28–30].

The previous studies on CT-guided mediastinal biopsy have reported a wide range of complication rates, from 3.8 to 25.5 % [22, 24, 29, 30]. The most frequently complication of mediastinal biopsy has been pneumothorax. In our study, the pneumothorax rate 3 % (3/100) was found to be lower than CT-guided TNB procedure. We believe that this low incidence of pneumothorax was possible, as the virtual navigation system enabled us to select a safer and more accurate targeting route in navigating the needle approach to the target. As for puncture approach, the transpulmonary approach was used for ten lesions to avoid damage to the lung tissue. In addition, the coaxial needle technique also played a significant role in the reduction of complications by avoiding repeated pleural punctures or passages. Of the three patients who had pneumothorax, all patients had pulmonary emphysema along the needle pathway, and this may suggest that considering emphysema in the needle pathway would be more likely to lead to the occurrence of pneumothorax. Considering the intrinsic disadvantage of CBCT, in which the large cone angle increases scattered radiation as well as noise, which in turn can disturb the discrimination of low-contrast objects, vascular injury during CBCT-guided PNB is of significant concern. However, after scrupulous review of the diagnostic contrast-enhanced CT data taken prior to the procedure, the estimation of the lesion boundary and the safe range for needle advancement was feasible [20]. An old patient with giant mediastinal lesion and upper vena cava compression syndrome occurred subcutaneous hemorrhage after procedure. Obstruction of superior vena cava leads to an increase in venous pressure, and injury to collateral vessels by puncture during procedure leads to subcutaneous bleeding. Puncture point was oppressed for 20 min, and bleeding was stopped.

There were four cases (4.3 %) misdiagnosed in the study. One patients' initial biopsy result was fibrous connective tissue; the nodule was enlarged more than 20 % in size on follow-up chest CT. TNB procedures were performed again, and the patient was confirmed with fibrosarcoma. The other there patients (one with HD and two with NHL) had completed the entire treatments, and tumor volumes were reduced more than 80 % compared with pretreatment. However, there were still persistence of soft tissue. Residual mediastinal tissue pathology results were coexists with fibrotic and/or necrotic tissue or thymic hyperplasia. Among them, two patients received the conventional open surgery and were confirmed with residual tumors. Another patient with NHL with high suspicion of tumor residue, TNB procedures were performed again and the patient was confirmed with residual tumor of NHL. An intrathoracic residual mass is present in 20 % of patients after treatment of an HD or an NHL. Eighteen percent of these patients experience a relapse at the level of the residual mass [31]. In our study, all patients were done with an enhanced chest CT before biopsy. CT alone does not allow one to discriminate between residual tumor and fibrosis or necrosis easily, especially for Lymphoma. According to most recent studies, CT has a poor sensitivity with respect to the diagnosis of residual disease. MRI has been shown to be slightly more reliable with respect to the diagnosis of fibrosis [32]. Preoperative MR combined with CT can better target mediastinal lesions and improve the correct rate. In fact, a negative result always possesses a diagnostic challenge. A non-specific benign result does not exclude malignancy, and further evaluation is required. The lesion may be malignant, but the sample obtained may lie outside the nodule borders or come from a necrotic area, thus preventing pathologists from establishing a correct diagnosis. Clinical and radiographic follow-ups are warranted. If further growth occurs after a non-specific benign diagnosis, it is obtained with TNB; repeat biopsy or resection is indicated [33].

In terms of radiation dose, a mean exposure dose was 9.7 ± 4.3 mSv. In Chiara et al. [18] study that dealt with pulmonary nodules with C-arm cone-beam CT, the total dose equals 11.62 mSv. Braak et al. [16] performed 92 biopsies in 88 patients with a similar guidance and reported a dose value equal to 9.95 mSv. On the basis of our results and the data from the literature regarding lung biopsies performed with CBCT guidance, despite the limited amount of currently available data and the lack of homogeneity, a slight reduction in dose could be hypothesized with the use of iGuide guidance. It could reduce the total dose delivered, because it can reduce the number of CBCT scans needed. The radiation dose of cone-beam CT-guided biopsy may not be a substantial problem, although a continuous effort must be made to reduce the radiation dose through use of a small field of view or collimation.

The limitations of this technique should also be mentioned. As patient movements may result in motion artifacts and affect the registration accuracy of the projected path, the key factor for achieving successful needle guidance is to generate high-quality 3D CBCT images. To this aim, during the imaging procedure, the patient should be well stabilized. However, this requirement may not be fulfilled and limits its applications for some patients who have difficulty sustaining a breath hold for the duration of imaging. The article did not have a control group, and it is difficult to assess the real advantages of CBCT-guided PNB for mediastinal lesions. Another main limitation of the study is the

small sample size that limits the statistical power. Future studies examining a larger population using this system are warranted in this regard.

In conclusion, flat detector cone-beam CT-guided PNB is an accurate and safe diagnostic method for mediastinal lesions.

Compliance with ethical standards

Conflict of interest The authors declare that they have no conflict of interest.

Research involving human participants All procedures performed in studies involving human participants were in accordance with the ethical standards of the institutional and/or national research committee and with the 1964 Helsinki declaration and its later amendments or comparable ethical standards.

Informed consent Informed consent was obtained from all individual participants included in the study.

Funding This study was funded by the National High-Tech Research and Development Program (863 Program) (Grant Number: 2015AA020301).

References

1. Lohr F, Georg D, Cozzi L et al (2014) Novel radiotherapy techniques for involved-field and involved-node treatment of mediastinal Hodgkin lymphoma: when should they be considered and which questions remain open? Strahlenther Onkol 190:864–866
2. Jiao D, Yuan H, Zhang Q et al (2015) Flat detector C-arm-guided transthoracic needle biopsy of small (≤2.0 cm) pulmonary nodules: diagnostic accuracy and complication in 100 patients. Radiol Med. doi:10.1007/s11547-015-0604-3
3. Gupta S, Seaberg K, Wallace MJ et al (2005) Imaging-guided percutaneous biopsy of mediastinal lesions: different approaches and anatomic considerations. Radiographics 25:763–786
4. Hiraki T, Mimura H, Gobara H et al (2009) CT fluoroscopy-guided biopsy of 1000 pulmonary lesions performed with 20-gauge coaxial cutting needles: diagnostic yield and risk factors for diagnostic failure. Chest 136:1612–1617
5. Priola AM, Priola SM, Cataldi A et al (2008) CT-guided percutaneous transthoracic biopsy in the diagnosis of mediastinal masses: evaluation of 73 procedures. Radiol Med. 113:3–15
6. Kim GR, Hur J, Lee SM et al (2011) CT fluoroscopy-guided lung biopsy versus conventional CT-guided lung biopsy: a prospective controlled study to assess radiation doses and diagnostic performance. Eur Radiol 21:232–239
7. Bissoli E, Bison L, Gioilis E et al (2003) Multislice CT fluoroscopy: technical principles, clinical applications and dosimetry. Radiol Med 106:201–212
8. Jin KN, Park CM, Goo JM et al (2010) Initial experience of percutaneous transthoracic needle biopsy of lung nodules using C-arm cone-beam CT systems. Eur Radiol 20:2108–2115
9. Lee SM, Park CM, Lee KH et al (2014) C-arm cone-Beam CT-guided percutaneous transthoracic needle biopsy of lung nodules: clinical experience in 1108 patients. Radiology 271:291–300
10. Wallace MJ, Kuo MD, Glaiberman C et al (2009) Three-dimensional C-arm cone-beam CT: applications in the interventional suite. J Vasc Interv Radiol 20:S523–S537
11. Hwang HS, Chung MJ, Lee JW et al (2010) C-arm cone-beam CT-guided percutaneous transthoracic lung biopsy: usefulness in evaluation of small pulmonary nodules. Am J Roentgenol 195:W400–W407
12. Cheung JY, Kim Y, Shim SS et al (2011) Combined fluoroscopy- and CT-guided transthoracic needle biopsy using a C-arm cone-beam CT system: comparison with fluoroscopy-guided biopsy. Korean J Radiol 12:89–96
13. Choi MJ, Kim Y, Hong YS et al (2012) Transthoracic needle biopsy using a C-arm cone-beam CT system: diagnostic accuracy and safety. Br J Radiol 85:e182–e187
14. Lee WJ, Chong S, Seo JS et al (2012) Transthoracic fine needle aspiration biopsy of the lungs using a C-arm cone-beam CT system: diagnostic accuracy and post-procedural complications. Br J Radiol 85:e217–e222
15. Choi JW, Park CM, Goo JM et al (2012) C-arm cone-beam CT-guided percutaneous transthoracic needle biopsy of small (≤ 20 mm) lung nodules: diagnostic accuracy and complications in 161 patients. Am J Roentgenol 199:W322–W330
16. Braak SJ, Herder GJ, van Heesewijk JP et al (2012) Pulmonary masses: initial results of cone-beam CT guidance with needle planning software for percutaneous lung biopsy. Cardiovasc Intervent Radiol 35:1414–1421
17. Choo JY, Park CM, Lee NK et al (2013) Percutaneous transthoracic needle biopsy of small (≤1 cm) lung nodules under C-arm cone-beam CT virtual navigation guidance. Eur Radiol 23:712–719
18. Floridi C, Muollo A, Fontana F et al (2014) C-arm cone-beam computed tomography needle path overlay for percutaneous biopsy of pulmonary nodules. Radiol Med. 119:820–827
19. Rotolo N, Floridi C, Imperatori A et al (2016) Comparison of cone-beam CT-guided and CT fluoroscopy-guided transthoracic needle biopsy of lung nodules. Eur Radiol 26:381–389
20. Kim H, Park CM, Lee SM et al (2015) C-arm cone-beam CT virtual navigation-guided percutaneous mediastinal mass biopsy: diagnostic accuracy and complications. Eur Radiol 25:3508–3517
21. Priola AM, Priola SM, Cataldi A et al (2008) CT-guided percutaneous transthoracic biopsy in the diagnosis of mediastinal masses: evaluation of 73 procedures. Radiol med 113:3–15
22. Kulkarni S, Kulkarni A, Roy D et al (2008) Percutaneous computed tomography-guided core biopsy for the diagnosis of mediastinal masses. Ann Thorac Med 3:13–17
23. De Margerie-Mellon C, de Bazelaire C, Amorim S et al (2015) Diagnostic yield and safety of computed tomography-guided mediastinal core needle biopsies. J Thorac Imaging 30:319–327
24. Petranovic M, Gilman MD, Muniappan A et al (2015) Diagnostic yield of CT-guided percutaneous transthoracic needle biopsy for diagnosis of anterior mediastinal masses. Am J Roentgenol 205:774–779
25. Gupta R, Cheung AC, Bartling SH et al (2008) Flat-panel volume CT: fundamental principles, technology, and applications. Radiographics 28:2009–2022
26. Busser WM, Braak SJ, Futterer JJ et al (2013) Cone beam CT guidance provides superior accuracy for complex needle paths compared with CT guidance. Br J Radiol 86:20130310
27. Brandén E, Wallgren S, Högberg H et al (2014) Computer tomography-guided core biopsies in a county hospital in Sweden: complication rate and diagnostic yield. Ann Thorac Med. 9:149–153
28. Schaefer PJ, Schaefer FK, Heller M et al (2007) CT fluoroscopy guided biopsy of small pulmonary and upper abdominal lesions: efficacy with a modified breathing technique. J Vasc Interv Radiol 18:1241–1248

29. Assaad MW, Pantanowitz L, Otis CN (2007) Diagnostic accuracy of image-guided percutaneous fine needle aspiration biopsy of the mediastinum. Diagn Cytopathol 35:705–709
30. Guimarães MD, Hochhegger B, Benveniste MF et al (2014) Improving CT-guided transthoracic biopsy of mediastinal lesions by diffusion-weighted magnetic resonance imaging. Clinics (Sao Paulo) 69:787–791
31. Gossot D, Girard P, Kerviler E (2001) Thoracoscopy or CT-guided biopsy for residual intrathoracic masses after treatment of lymphoma. Chest 120:289–294
32. Garnon J, Ramamurthy N, Caudrelier JJ et al (2015) MRI-guided percutaneous biopsy of mediastinal masses using a large bore magnet: technical feasibility. Cardiovasc Intervent Radiol. doi:10.1007/s00270-015-1246-5
33. Jiao DC, Li ZM, Yuan HF (2016) Flat detector C-arm CT-guidance system in performing percutaneous transthoracic needle biopsy of small (≤3 cm) pulmonary lesions. Acta Radiol 57:677–683